



HAL
open science

Advances in microclimate ecology arising from remote sensing

Florian Zellweger, Pieter de Frenne, Jonathan Roger Michel Henri Lenoir,
Duccio Rocchini, David Coomes

► **To cite this version:**

Florian Zellweger, Pieter de Frenne, Jonathan Roger Michel Henri Lenoir, Duccio Rocchini, David Coomes. Advances in microclimate ecology arising from remote sensing. Trends in Ecology & Evolution, 2019, 34 (4), pp.327-341. 10.1016/j.tree.2018.12.012 . hal-02352615

HAL Id: hal-02352615

<https://hal.science/hal-02352615>

Submitted on 16 Nov 2019

HAL is a multi-disciplinary open access archive for the deposit and dissemination of scientific research documents, whether they are published or not. The documents may come from teaching and research institutions in France or abroad, or from public or private research centers.

L'archive ouverte pluridisciplinaire **HAL**, est destinée au dépôt et à la diffusion de documents scientifiques de niveau recherche, publiés ou non, émanant des établissements d'enseignement et de recherche français ou étrangers, des laboratoires publics ou privés.

1 Advances in microclimate ecology arising from remote
2 sensing

3
4 Florian Zellweger¹, Pieter De Frenne², Jonathan Lenoir³, Duccio Rocchini^{4,5,6},
5 David Coomes¹

6
7 ¹ Forest Ecology and Conservation Group, Department of Plant Sciences, University of Cambridge, Downing
8 Street, Cambridge CB23EA, UK

9 ²Forest & Nature Lab, Ghent University, Geraardsbergsesteenweg 267, BE-9090 Gontrode, Belgium

10 ³ UR “Ecologie et dynamique des systems anthropisés” (EDYSAN, UMR 7058 CNRS-UPJV), Université de
11 Picardie Jules Verne, 1 Rue des Louvels, 80037 Amiens Cedex 1, France

12 ⁴ University of Trento, Center Agriculture Food Environment, Via E. Mach 1, 38010 S. Michele all'Adige (TN),
13 Italy

14 ⁵ University of Trento, Centre for Integrative Biology, Via Sommarive, 14, 38123 Povo (TN), Italy

15 ⁶Fondazione Edmund Mach, Research and Innovation Centre, Department of Biodiversity and Molecular
16 Ecology, Via E. Mach 1, 38010 S. Michele all'Adige (TN), Italy

17
18 Correspondence: fz255@cam.ac.uk (Zellweger, F.); dac18@cam.ac.uk (Coomes, D.)

19 **Keywords:** Biodiversity, Climate Change Ecology, Light Detection and Ranging LiDAR,
20 Thermal imaging, Topography, Vegetation Cover

21

22 **Abstract**

23 Microclimates at the land-air interface affect the physiological functioning of organisms
24 which, in turn, influences the structure, composition and functioning of ecosystems. We
25 review how remote sensing technologies that deliver detailed data about the structure and
26 thermal composition of environments are improving the assessment of microclimate over
27 space and time. Mapping landscape-level heterogeneity of microclimate advances our ability
28 to study how organisms respond to climate variation, which has important implications for
29 understanding climate-change impacts on biodiversity and ecosystems. Interpolating in-situ
30 microclimate measurements and downscaling macroclimate provide an organism-centred
31 perspective for studying climate-species interactions and species distribution dynamics. We
32 envisage that mapping of microclimate will soon become commonplace, enabling more
33 reliable predictions of species and ecosystem responses to global change.

34 **Importance of microclimate maps**

35 Local modification of the **climate** (See Glossary) by topography and vegetation produces
36 **microclimates** at the land-air interface which can differ greatly from the climatic means [1,2].
37 Surface temperatures between north- and south-facing mountainsides, for example, can vary
38 by 20 °C, equivalent to a latitudinal gradient of about 2000 km [3]. Additionally, forest
39 canopies can buffer the diurnal amplitude of air temperature in the forest **understorey** by 7
40 °C [4]. Such differences in temperature within landscapes matter to organisms, affecting
41 processes such as respiration, heat and energy exchange which, in turn, set thermodynamic
42 constraints on species behaviour, growth, reproduction and survival [5–7]. Innumerable
43 papers over the past century have quantified microclimates and their influences on ecological
44 processes at all levels of organization, from physiological processes of single organisms to
45 ecosystem-level productivity and nutrient cycling [4–6,8–10]. Microclimate is also relevant to
46 evolution because phenotypic and genotypic adaptations are driven by environmental
47 conditions actually experienced by the organisms [11]. Moreover, microclimate mapping and
48 monitoring have been recognised as key to effective natural resource management, with
49 forestry, agroforestry and agriculture being prominent examples [6,12].

50 Microclimate ecology is attracting renewed attention due to its fundamental importance
51 in understanding how organisms respond to climate change [2]. Species distributions are
52 typically modelled using **macroclimate** data obtained from national networks of weather
53 stations [13,14]. These standard meteorological data are measured in open areas at 1.5 - 2 m
54 height above short grass, and capture synoptic conditions that are unrepresentative of a range
55 of microclimates that most organisms experience [15,16]. These inaccuracies and biases can
56 have serious implications when predicting organismal responses to climate change. For
57 example, recent studies suggest that many plant and animal communities are accumulating a
58 **climatic debt** because they are migrating more slowly than needed to keep up with
59 macroclimate warming [17–22]. However, **temperature buffering** near the ground – due to

60 local radiation regimes, soil characteristics and topography – means that organisms may not
61 have to migrate, or adapt, as quickly as previously thought to keep pace with the shifting
62 macroclimate [23,24] (Box 1). Thus, extinction risk from climate change for plants and
63 insects is considerably reduced by the occurrence of **microrefugia** within landscapes with
64 highly heterogeneous microclimate [25]. Yet, the modulating effects of microclimate
65 variability on climate change impacts have only recently started to be quantified [3,21,25–29].

66 A key impediment to progress in incorporating microclimate into models of climate
67 change impacts on organisms has been our limited ability to map and monitor microclimatic
68 variation over large spatial scales and over time. Networks of microclimate sensor provide
69 point-based measurements and weather stations provide macroclimate data, but we have
70 lacked approaches to effectively interpolate and downscale this information. **Remote sensing**
71 is now offering opportunities to lift this technical barrier, by producing detailed and spatially
72 continuous data-layers that can be used as explanatory variables to understand and model the
73 horizontal and vertical variation in microclimatic conditions over large spatial and temporal
74 scales. Here, we review how these emerging technologies are advancing microclimate
75 modelling and mapping, and highlight some of the opportunities they provide for ecology,
76 conservation and climate change research.

77 **Box 1 Shifts in species distributions in response to global warming**

78 Microclimate – the local modulation of macroclimate by vegetation canopies and topographic position
79 – affects species re-distribution under climate change (Figure I). Maps of microclimate predicted from
80 remote sensing data can improve habitat suitability maps and predictions of how species will respond
81 to climate change.

82

83 **Eureka: remote sensing advances for modelling and mapping microclimate**

84 Remote sensing technologies are increasingly capable of mapping the structural complexity
85 and thermal composition at the ground-atmosphere boundary at scales relevant to studying

86 organismal responses to environmental variation [27]. We discuss the contributions that laser
87 scanning, photogrammetry, hyperspectral imaging and thermal imaging are making.

88 **Airborne Light Detection and Ranging (LiDAR)** (aka airborne laser scanning) is
89 particularly valuable for modelling and mapping microclimate because it provides spatially
90 continuous, sub-metre-scale information on two key modifiers of climate at the ground-
91 atmosphere interface: ground topography and vegetation structure [30]. To construct maps,
92 microclimate measurements taken on the ground using sensor networks are related to LiDAR
93 structural information, such as topographic position and light incidence at very high
94 resolutions (Boxes 2-4), using statistical modelling approaches, and the function generated by
95 this approach is then used to predict microclimate across the entire LiDAR-mapped landscape
96 (Figure 1) [13,31–35]. Effective interpolation requires that the sensor networks sample
97 contrasting sites within the study area. The sensor data must also be summarised in
98 ecologically meaningful ways, guided by clear research questions [36]. For example, the
99 frequency of extremely cold or hot temperatures, calculated over timescales relevant for the
100 growth and survival of organisms, are more meaningful for biogeographic applications than
101 average conditions [2,36].

102 Aerial photography provides an alternative approach to assessing topography and forest
103 structure, using photogrammetry and structure-from-motion (SfM) techniques to construct 3D
104 surfaces (Figure 2) [37]. These inexpensive and easy-to-use methods are increasingly applied,
105 but are less accurate than LiDAR at deriving terrain elevation beneath tree canopies, or for
106 measuring vertical vegetation structure, because photos only record reflectance off the upper
107 surface [38,39]. One-off mapping of large areas using LiDAR and aerial photography is
108 normally conducted from manned aircrafts, while unmanned aerial vehicles (UAV, e.g.
109 drones) equipped with miniaturised cameras and LiDAR sensors are becoming available to
110 map smaller areas at even higher spatiotemporal resolutions. Using UAVs and SfM
111 techniques, Milling et al. [40] found that summer maximum temperatures may vary up to four

112 degrees Celsius over just a few metres within sagebrush-steppe landscapes – habitats that
113 were previously considered relatively homogeneous. A key advantage of UAVs is that
114 deployment is very flexible, enabling the collection of time-series of aerial imagery over a
115 period of interest at relatively low costs. SfM techniques applied to image time-series offer
116 novel opportunities for monitoring microclimate in ecosystems in which phenology creates
117 strong temporal variation in microclimate [41,42].

118 **Terrestrial laser scanning (TLS)** provides immensely detailed datasets of vegetation
119 structure that can be used to model microclimate. Complementary to airborne laser scanning,
120 which maps 3D vegetation structure from above, TLS maps vegetation in extraordinary detail
121 from below, thus providing information on the understorey structure. Kong et al. [43] found
122 that TLS-based reconstructions of canopy volumes coupled with microclimate measurements
123 revealed cooling effects in the understorey that varied among tree species, suggesting that
124 TLS can pick up subtle effects of different leaf sizes on understorey microclimate. Moreover,
125 Ehbrecht et al. [44] found that TLS-derived measurements of canopy openness were
126 positively related to diurnal temperature ranges in managed temperate forests in Germany.
127 TLS measurements are restricted to a few hectares and are of limited use, compared to
128 airborne laser scanning, for modelling microclimate over large areas. Yet, the forest
129 understorey-structure information TLS provides at the plot level has been shown to improve
130 landscape-level vertical vegetation structure mapping based on full-waveform airborne
131 LiDAR [45].

132 Complementing maps of 3D vegetation structure, maps of leaf functional traits and
133 species obtained by **hyperspectral remote sensing** [46,47] are likely to improve the
134 statistical fit of microclimate models. We expect this improvement because the quality and
135 quantity of solar radiation transmitted by canopies vary according to leaf traits and tree
136 species, leading to species-specific microclimatic conditions in the understorey [48].

137 However, we are unaware of studies using hyperspectral remote sensing to map microclimate
138 (see Outstanding Questions).

139 **Box 2: Measuring how plant canopies affect solar radiation fluxes**

140 Solar radiation flux has strong effects on the energy budget and performance of organisms living
141 beneath vegetation canopies. Radiation regimes along the vertical canopy profile of forests can be
142 estimated from a Light Detection and Ranging (LiDAR) point cloud by creating a 3D map of foliage
143 presence/absence in voxels (i.e. 3D pixels) and then apply ray tracing algorithms to evaluate whether
144 beams entering the canopy in different locations and angles are likely to be intercepted [31,49].
145 Alternatively, LiDAR data can be used to generate synthetic hemispherical images from which fluxes
146 of non-directional diffuse sky radiation and direct solar radiation, or light extinction following the
147 Beer-Lambert law [50], can be calculated for any time in the day or year (Figure I). These approaches
148 are computationally intensive but better represent light conditions experienced by forest organisms
149 than simple approaches based on canopy cover [51]. Vegetation structure thus drives the interception
150 of solar radiation, which means that the importance of vegetation structure for microclimate will vary
151 between day and night and different weather conditions, with the temperature offsets highest on bright
152 sunny days. Advances in physically based radiative transfer modelling now make it possible to
153 estimate the 3D radiative budget in forests and open lands at an ever-increasing detail, e.g. by
154 accounting for foliar-specific filtering of different wavelengths [52].

155 **Box 3: Temperature buffering and offset**

156 Solar radiation reaching the land-atmosphere interface is mostly reflected, or absorbed and re-emitted
157 as thermal radiation, or drives evapotranspiration. Vegetation canopies lift energy-exchange surfaces
158 off the ground, and in doing so modulate radiant fluxes, air temperature and humidity at ground level.
159 The capacity of plant canopies to sustain a different temperature below canopy compared to free-air
160 conditions (i.e. a temperature offset) is thus closely related to canopy structure and composition.
161 Under canopy, diurnal changes in temperatures are less extreme than above canopy, and this
162 temperature buffering is modulated by canopy height and cover, both of which can now be precisely
163 mapped [13,32,53].

164 Sensor networks sampling environmental gradients (*cf.* Figure 1) are increasingly combined
165 with remote sensing data to map microclimate. The current scientific literature often makes crude
166 assumptions about the shading and temperature buffering effect of vegetation when modelling
167 microclimate, and usually neglects systematic changes in the temperature offset over time, i.e. the
168 offset trend (Figure 1) [24,28]. The degree to which temperatures below the canopy are offset
169 compared to free-air conditions will not be constant over time and depend on successional processes
170 driving dynamics in canopy structure and composition. Long time series of below-canopy temperature
171 records thus need to be related to forest dynamics to better understand the drivers of long-term
172 microclimatic dynamics [24]. Such data are scarcely available [54] and global long-term networks
173 such as FLUXNET may prove very valuable in this respect.

174 Forest microclimates are also affected by landscape features such as distances to forest edges,
175 urban areas and large water bodies. Many of these landscape features can be retrieved from remote
176 sensing data [4,29,32,35,55] and integrated into predictive models used to map microclimate. Another
177 key influence on spatiotemporal dynamics in microclimate is topographic position, because it
178 determines the influences of **cold air drainage** and pooling on a site [56,57]. Topographic position
179 and cold air drainage can be estimated from high-resolution digital terrain models (DTMs), further
180 increasing our ability to map and model microclimate across broad spatial and temporal scales.

181

182

183

184 **Box 4: Water and wind**

185 Plant canopies not only buffer temperature, but also precipitation, relative humidity and **vapour**
186 **pressure deficit (VPD)**, which is exponentially related to air temperature. VPD drives transpiration in
187 plants and growth and survival can be impeded when VPD is high (responses vary greatly among
188 species and depend on water supply and leaf temperature). In a degraded tropical forest landscape,
189 models of understorey VPD generated by interpolating sensor-network data with LiDAR imagery (see
190 Figure 1) suggest that tropical tree regeneration will be severely affected by global warming, because
191 of the close link between temperature and VPD [13]. The effect of remotely sensed canopy structure
192 and composition on below-canopy VPD and moisture availability warrants further research, e.g. to
193 better understand how moisture influences air and topsoil temperatures, and *vice-versa* [31,58].

194 Topographic features, such as slope angle, affect the lateral surface and subsurface water flow.
195 Airborne LiDAR-derived maps of topographic wetness and ruggedness are thus suitable to analyse the
196 fine-scale variation of soil moisture and air humidity [59,60]. Detailed ecosystem structure data also
197 delivers input parameters to better account for the effects of wind on microclimate. Canopy surface
198 roughness and vertical canopy structure, for instance, improve wind modelling in heterogeneous
199 forests and offer promising opportunities to make predictions of the near-surface wind fields more
200 accurate [61,62].

201

202 **Thermal imaging** using thermal infrared (TIR) cameras can be applied to map surface
203 temperatures. As opposed to LiDAR technologies TIR cameras directly record longwave
204 infrared radiation (i.e. 7.5-14 μm) emitted by an object or organism, which is linked to surface
205 temperature according to Boltzmann's law when surfaces have high emissivity [3,63]. The
206 surface and body temperature of an organism is related to its energy budget and thus to the
207 functioning and performance of plants and animals [7,64]. Yet, the surface temperature is not
208 necessarily related to the air temperature an organism experiences. For instance, plants
209 respond to water shortage by closing stomata and reducing transpiration, which causes leaf

210 surface temperatures to rise – irrigated and non-irrigated plants can differ in leaf temperature
211 by several degrees but have similar air temperature in their surrounds, as measured with
212 shielded temperature sensors (Figure 2). TIR images recorded by UAVs have centimetre
213 resolution [63], providing valuable means for the fine-scale monitoring and management of
214 water use and water stress by plants, e.g. in crop production [66,66], or to assess the
215 temperature experienced by insects living on a leaf’s surface. However, TIR images might not
216 necessarily reflect atmospheric or soil microclimatic temperatures experienced by plants, i.e.
217 their thermal niche.

218 Surface temperatures from high-resolution TIR images have been applied for fire and
219 disease detection, phenotyping in plant breeding, wildlife monitoring and microclimate
220 ecology (reviewed in [42,66]). Senior et al. [67], for example, used TIR images to show that
221 selective logging of tropical forests had a very little impact on thermal buffering compared to
222 primary forests, suggesting that selectively-logged tropical forests may play an important role
223 in retaining species with temperature niches that are disappearing under climate change. In
224 aquatic systems, TIR images provide the means for landscape-level mapping of cold water
225 patches (thermal refuges) along rivers – an important habitat element for riverine salmonids in
226 times of climate warming [68]. Such maps provide valuable information to guide conservation
227 efforts. We currently know little about the extent to which canopy surface temperatures
228 measured by TIR images are coupled to the temperatures prevailing in the layers beneath the
229 canopy surface, e.g. in forest understoreys or at the soil surface, although this knowledge
230 would be helpful for using TIR images to model and map microclimatic air temperature. The
231 difference between canopy leaf temperatures and ambient air temperatures can be highly
232 variable and depends on canopy structure and species-specific leaf traits, such as aerodynamic
233 leaf boundary-layer resistance and associated levels of atmospheric coupling [69]. Such
234 analysis will also be subject to effects deriving from the ability of plants to regulate leaf
235 temperature [64]. Research into the relationship between below-canopy temperatures

236 measured by sensor networks (Box 3) and canopy temperature measured by TIR images is
237 needed to further understanding of these linkages.

238 TIR radiation flux is affected by a number of factors besides leaf temperature, including
239 the relative humidity, ambient temperature, wavelength dependency of the emissivity and
240 range of the camera, wind speed and shadows [70]. Accurate surface temperature assessments
241 using TIR imagery can thus be challenging. A key point is the emissivity, which is the ability
242 of the surface of an object to emit thermal radiation [63,71]. The mean emissivity of surfaces
243 from plants, soil and rocks range from 0.903-0.997 and deriving surface temperature data
244 from TIR images is thus complicated by the fact that not all surfaces in the image have similar
245 thermal emissivity [71]. Furthermore, the spatiotemporal resolution of TIR imagery needs to
246 be considered. Representing the climate conditions at a site requires TIR images taken across
247 the full range of weather conditions, at day and night, and across seasons [2]. While this may
248 be feasible for terrestrial and potentially airborne TIR imagery, the high spatiotemporal
249 resolution of such datasets comes at the cost of limited spatial coverage. Satellite TIR imagery
250 provides surface temperature data with global coverage, although at too coarse a resolution to
251 directly quantify microclimate (Figure 2). Yet, satellite TIR images can improve the
252 interpolations of temperature data from weather stations in areas with a low station density
253 [72]. Despite these challenges and limitations, the potential of TIR imagery in fundamental
254 and applied microclimate ecology is substantial and should be explored in more detail.

255 Another approach to microclimate mapping is to downscale macroclimate data obtained
256 from macroclimatic grids [2,24], such as WorldClim 2 [72] and CHELSA [73], which are
257 published at relatively coarse scales (typically 30'' resolution, equivalent to 1 km² at the
258 equator). High-resolution remote sensing products, such as **digital terrain models** (DTMs),
259 **canopy height models** (CHMs) or detailed ground and canopy albedo measurements, are
260 used to generate indices of microclimatic processes related to solar radiation, cold-air
261 drainage or topographic wetness from the grid data, and these indices are then related

262 statistically to macroclimatic variables using regression [74–76]. Software such as R-packages
263 implementing these approaches using freely available input data are now becoming available
264 [14]. Because these models are based on macroclimate data that are available at a high
265 temporal resolution, such models allow for predictions of how microclimate conditions vary
266 in time, thus tackling a key limitation of temporally limited approaches based on microclimate
267 measurements from sensor networks (*cf.* Box 3).

268 Mechanistic models may also use predictor variables derived from remote sensing data
269 but are fundamentally different in that they model heat and mass exchange between organisms
270 and their environments, relying on functional relationships derived from the physical
271 processes involved in creating microclimate [77,78]. Perhaps the most advanced mechanistic
272 model is Niche MapperTM [77], which downscales air temperatures based on a set of abiotic
273 variables such as soil characteristics, macroclimatic meteorological variables including cloud
274 cover, air temperatures and wind speeds and shading. The model has been parameterized to
275 predict lizard distributions in open habitats in Australia and the US but does not currently
276 include detailed modulating influences of plant canopies among its input variables [28,77].

277 **Implications and avenues for microclimate ecology**

278 Ecologists are starting to appreciate the ways in which microclimate mapping technologies
279 could improve their science. Correlative species distribution modelling (SDM) is often
280 criticised for its reliance on coarse climate information [24] and its failure to incorporate
281 physiological knowledge [8]. Using detailed spatiotemporal microclimate data in such models
282 will allow for more organism-centred approaches to determine species range boundaries and
283 their climate change-related dynamics. This especially applies at the temperature-driven
284 leading and trailing edges, where the response of organisms may be particularly susceptible to
285 the availability of suitable microclimate and associated microrefugia [8,24,26,79,80].
286 Incorporating microclimate layers into SDMs thus holds a large potential, but is still in its

287 infancy. Using simulations and focusing on maximum temperature of the warmest month,
288 Lenoir et al. [24] found that using airborne LiDAR-derived variables to model microclimate
289 decreases the extirpation risk of a virtual plant species under climate change compared to
290 predictions based on downscaled climate data at coarser resolutions (Box 1). Such modelling
291 results are physiologically more meaningful because they derive from the comparison of the
292 species' temperature niche to realistic temperature dynamics driven by vegetation shading and
293 cold air drainage.

294 Microclimate data will also help to shed new light into microclimatic effects on
295 phenology – potentially quantified by remotely sensed vegetation indices such as the
296 Normalized Difference Vegetation Index (NDVI) – and how these effects affect species
297 distributions and species interactions. For instance, plant species range limits may be driven
298 by temperature extremes during key stages of phenology, such as extreme cold during bud-
299 break of broad-leaved tree species [81]. Such extreme events are not represented in currently
300 available climate data with coarse spatiotemporal resolutions. Using remote sensing data to
301 derive climate data at resolutions similar to those at which organisms perceive and respond to
302 climate conditions is thus a timely task and will pave the way for more reliable predictions of
303 species range dynamics in response to climate change [27].

304 Microclimate mapping could also refine our understanding of species diversity patterns.
305 Following the environmental heterogeneity hypothesis, microclimate heterogeneity is
306 expected to be positively related to species richness (**alpha diversity**) [82], but this remains
307 understudied. Similarly, investigating how spatial and/or temporal changes in microclimate
308 contributes to **beta diversity** through environmental filtering deserves more attention [82,83].
309 For example, a recent study found that microclimate on cooler, north-facing slopes affected
310 plant community responses to climate change by delaying extinctions of species with low-
311 temperature requirements [84]. Increased short distance microclimatic variation is expected to
312 affect the climatic debt in bird assemblages, e.g. by lowering the risk of population decline

313 due to the ability to avoid harmful climatic variation or by increasing landscape permeability
314 which facilitates the spatial tracking of climate change [85]. Spatiotemporal mapping of
315 microclimate will thus be crucial to understanding how local phenomena give rise to large-
316 scale processes. Estimating connectivity among fragmented habitats to evaluate the
317 functionality of ecological networks, for instance, depends on reliable landscape-level
318 representations of microrefugia, stepping stones, 3D-habitat structure and associated
319 microclimate (e.g. ecological corridors such as hedgerows), as these attributes are critical for
320 species migration and gene flow [79,80,86].

321 The potential of remote sensing technologies to better understand and model
322 microclimate is already recognised implicitly in the ecological literature. The widespread use
323 of LiDAR to model species occurrence from habitat structure, for instance, relies implicitly on
324 the assumption that LiDAR data can be used to assess microclimate conditions that are, at
325 least partially, responsible for the fitness and distribution of an organism [87–89]. What is
326 missing in such indirect approaches is how the measured environmental features actually
327 drive and interact with the microclimate variables that are physiologically relevant to the
328 species or the biological phenomena of interest, e.g. the minimum and maximum air
329 temperatures relevant to an organism’s temperature tolerance [7]. In forests, our mechanistic
330 understanding of how canopy structure and composition drive and interact with vertical
331 radiation and temperature regimes to determine species habitat preferences and vertical niche
332 partitioning is still incomplete. Indeed, the steep vertical microclimatic gradients within
333 forests are increasingly appreciated for structuring arboreal biodiversity, particularly in the
334 tropics [90–92] and the remote sensing approaches described here play a key role in filling
335 this knowledge gap.

336 Microclimatic changes arising from forest management have been shown to exert strong
337 controls on local plant communities and their response to macroclimate warming [21]. Thus,
338 mapping of microclimate has far-reaching implications for conservation and other fields, such

339 as forestry and agriculture [35]. Successful tree regeneration – planted or natural – strongly
340 depends on microclimate conditions [12,74]. Maps of thermal and light regimes below
341 different canopy conditions or in clear-cuts can help managers optimise planting in
342 accordance to tree species-specific temperature and light adaptations [12]. Similarly,
343 microclimate maps would be helpful for managing agroforestry systems, such as those
344 associated with coffee and cacao, where microclimates affect yield and the susceptibility to
345 climate extremes [93]. In agriculture, precision farming of speciality crops increasingly relies
346 on remote sensing technologies capturing the spatiotemporal variability of the micro-
347 environmental conditions [94,95]. Mapping the thermal heterogeneity across landscapes
348 improve the analysis and management of crop water status [66,94] and how microclimate
349 affects the occurrence and dynamics of pests [63,96].

350 **Current limitations and future directions**

351 Field measurements of microclimate recorded with sensor networks are crucial for the
352 development of landscape-scale maps, but sensor and sampling designs vary greatly between
353 studies, making it difficult to synthesise results [2]. The need for standardised sampling
354 approaches, centred around the following principles, is increasingly recognised: (1) field
355 surveys are designed to represent the entire spatial and temporal gradients of the microclimate
356 conditions in the study system; (2) time span between the collection of field and remote
357 sensing datasets is short enough to prevent significant discrepancies; and (3) measurement
358 sites are georeferenced precisely using a differential Global Positioning System, so that the
359 data can be spatially co-registered with the imagery. Simulations show that registration errors
360 as small as 1 m when working with 10-m radius plots can create major uncertainty in forest
361 properties estimated from airborne LiDAR [97]. Thus, also precisely locating species records,
362 particularly of less mobile species, is a prerequisite for sound inference about species-
363 microclimate relationships.

364 The presented airborne remote sensing tools and data (i.e. involving airborne LiDAR
365 and/or SfM) to map the effects of vegetation structure on microclimate near the ground work
366 best in tall habitats, such as forests, wood- and shrublands. In short stature vegetation, such as
367 grassland, heath or crops, the level of structural detail picked up by airborne LiDAR and SfM
368 is unlikely to capture microclimate variation resulting from fine-scale differences in
369 vegetation structure. High-resolution TIR, however, provides the means to measure surface
370 temperatures in both tall and short stature vegetation, but does not provide structural
371 information required to interpolate microclimate measurements from sensor networks.

372 There is pressing need to gather georeferenced microclimate data from different types of
373 habitat across the globe and a global archive and data portal facilitating data access would
374 significantly promote progress in microclimate ecology. To complement temporal dynamics
375 of microclimate data gained from downscaled macroclimate we need long-term microclimate
376 data series [24]. This will enable an improved understanding of the drivers of microclimate
377 dynamics and how they deviate from the macroclimate, which will have important
378 implications for estimating the velocity, and thus impact, of climate change.

379 Many of the remote sensing approaches described here rely on data whose spatial
380 coverage is growing but does not yet expand over continental and global scales. In the future,
381 remedial satellite LiDAR data experiments, e.g. the Global Ecosystem Dynamics
382 Investigation LiDAR (GEDI) or the ICESat-2 satellite project, may provide new avenues to
383 arrive at analysing and monitoring microclimate variation at larger temporal and spatial
384 scales. Satellite missions employing synthetic aperture radar (SAR) systems, such as the
385 launched TanDEM-X and planned Tandem-L missions, provide worldwide, repeated and
386 spatially detailed data for digital terrain elevation and forest height modelling. Incorporating
387 these data into microclimate models may play a key role for increasing their spatial and
388 temporal cover, and is expected to facilitate tracking microclimatic changes in habitats with
389 dynamic structural attributes, such as forest vegetation structure.

390 **Concluding Remarks**

391 We have shown that advances in remote sensing technologies are making it possible to map
392 microclimate at fine spatiotemporal resolutions and over large areas for the first time. This
393 offers new opportunities to scale up ecological knowledge about the organism-environment
394 interactions at fine scales, to understand species and ecosystem responses to environmental
395 changes over broad scales.

396 Topographically controlled microclimate gradients have historically been studied in
397 more detail than those controlled by 3D-vegetation structure. LiDAR and photogrammetry
398 provide key structural data to fill this gap, which is critical, given the contribution that
399 vegetation structure makes to biodiversity. However, methodological efforts taking an
400 ecological perspective in approximating microclimate via remote sensing tools are required to
401 make most out of the available data and resources. The technological advances in remote
402 sensing and the methodological advances in microclimate modelling call for coordinated
403 efforts between remote sensing experts, climatologists and ecologists to improve our
404 predictive abilities on the role of microclimate in biodiversity and global change ecology.

405

406

Outstanding questions

407 Improved, open-access and easy-to-use methods based on remotely sensed canopy structure and
408 composition for modelling and predicting microclimate in forests are needed. Such methods are
409 required to further our understanding of light, temperature and relative humidity regimes, and how
410 they affect species behaviour, performance and distribution. Emphasis should also be given to
411 quantifying the effect of local wind dynamics on microclimate.

412

413 How will microclimatic conditions change in response to climate warming? This will depend on the
414 extent to which vegetation structure and topography modulate air temperature and how changes in
415 vegetation structure change solar radiation and wind regimes.

416

417 How does horizontal and vertical microclimate variation affect alpha- and beta-diversity?

418

419 What is the influence of microclimate buffering on species range dynamics, biodiversity and the
420 climatic debt of species and communities?

421

422 How are microclimate gradients related to plant functional traits derived from hyperspectral imaging?

423

424 How could landscape-level mapping of microclimate contribute to our understanding of habitat
425 connectivity and the functionality of ecological networks?

426

427 How are below canopy and soil microclimate linked to vegetation surface temperatures measured by
428 thermal infrared (TIR) imagery?

429

430 How important is microclimate for driving phenological responses to climate change, and what are the
431 implications thereof for species interactions and distributions?

432

434 **Glossary**

435 **Airborne LiDAR:** a remote sensing technology used for 3D analysis of earth surface environments.
436 LiDAR is short for Light Detection and Ranging (aka laser scanning). A LiDAR sensor emits about
437 200,000 laser pulses per second towards the ground and measures the energy waveform returning from
438 backscattering objects. When used to measure vegetation structure, the light pulse is wider than a
439 typical leaf by the time it reaches the upper canopy, meaning that some of its energy passes through
440 the upper canopy to lower layers and even the ground. The sensor converts the continuous waveform
441 of returning energy into ‘discreet returns’ and, by precisely recording return times and its location in
442 the air, creates a 3D point cloud of the position of objects. The point cloud is used to derive high-
443 resolution of topography and canopy height (see DTM and CHM) and detailed information on vertical
444 vegetation structure, spatially continuous across large areas. Some LiDAR sensors record the full-
445 waveform, providing detailed information about the entire vertical forest profile. The added value of
446 full-waveform over discrete LiDAR for microclimate mapping remains to be tested.

447 **Alpha diversity:** species diversity in sites or habitats at the local scale (e.g. point-based surveys),
448 often expressed as the total number of species (species richness) or abundances weighted indices, such
449 as the Shannon index or the Simpson index.

450 **Beta diversity:** diversity measure expressing variation (turnover and nestedness) in community
451 composition among habitats gradients, can be calculated based on taxonomic (e.g., species identities),
452 functional (e.g., functional traits) and phylogenetic (e.g., branches) units.

453 **Canopy Height Model (CHM):** continuous digital surface – usually in the form of a raster dataset –
454 representing the height of the canopy above the underlying terrain.

455 **Climate:** synthesis of atmospheric conditions characteristic of a particular place in the long-term
456 (usually 30-year averages) expressed by averages of various elements of weather and probabilities
457 distributions of extreme events.

458 **Climate debt:** biotic responses observed in nature are often slower than expected under the
459 assumption of complete synchrony with climate change; climate debt describes the spatiotemporal lag

460 accumulated by a species or a community compared to the actual shift in climate.

461 **Cold air drainage:** gravity-induced, downslope flow of relatively cold air near the ground, pooling in
462 local depressions and valley constrictions. A prominent phenomenon in mountain valleys at night and
463 during winter.

464 **Digital Terrain Model (DTM):** continuous digital surface representing the elevation height of the
465 bare earth. Sometimes also referred to as digital elevation model (DEM).

466 **Hyperspectral remote sensing:** image analysis based on the spectral reflectance across a wide range
467 of the electromagnetic spectrum; also known as hyperspectral imaging or imaging spectroscopy.

468 **Macroclimate:** the climate conditions above ground or above the canopy (e.g. > 2 m) at a relatively
469 large scale, e.g. across spatial dimensions of 1 km or more, and temporal dimensions of days to weeks
470 or longer.

471 **Microclimate:** the climate conditions close to the ground (e.g. < 2 m) or along vertical forest profiles
472 at relatively fine spatiotemporal resolutions, e.g., across spatial dimensions of centimetres to meters,
473 and temporal dimensions of minutes or shorter. Microclimate conditions include temperature,
474 precipitation, humidity, wind and radiation regimes.

475 **Microrefugia:** spatially-restricted local habitats that sustain a climate that has become, or is
476 becoming, lost due to climate change and that enables species to persist in an otherwise inhospitable
477 region.

478 **Remote sensing:** acquiring information about an object of phenomena from a distance.

479 **Temperature buffering:** below plant, especially forest canopies, daily air temperatures may be
480 substantially buffered, increasing less during the day and decreasing less during the night than outside
481 the forest canopies.

482 **Terrestrial Laser Scanning (TLS):** the process of gathering 3D data using a LiDAR instrument on
483 the ground. 3D point clouds produced by TLS are typically much denser than those obtained by
484 airborne LiDAR.

485 **Thermal imaging:** technique to produce an image based on the heat emitted by an object or an
486 organism.

487 **Understorey:** a layer of vegetation close to the floor beneath the main canopy of a forest.

488 **Vapour pressure deficit (VPD):** the difference between saturation vapour pressure and the actual
489 vapour pressure, at a given temperature.

490

491 **Acknowledgements**

492 FZ was funded by the Swiss National Science Foundation (grant no. 172198). PDF received
493 funding from the European Research Council (ERC) under the European Union's Horizon
494 2020 research and innovation programme (ERC Starting Grant FORMICA 757833). DR was
495 partially funded by the the H2020 project ECOPotential (Grant Agreement no. 641762)
496 and the H2020 TRuStEE - Training on Remote Sensing for Ecosystem modElling project
497 (Grant Agreement no. 721995). DAC was funded by NERC (grant number NE/K016377/1)
498 and a Leverhulme International Fellowship. We thank the Swiss NFI for providing LiDAR
499 data and two anonymous reviewers and Christian Körner for commenting on earlier versions
500 of the manuscript.

501

502 **References**

- 503 1 Geiger, R. *et al.* (2003) *The climate near the ground*, Rowman and Littlefield, Oxford.
- 504 2 Bramer, I. *et al.* (2018) Advances in Monitoring and Modelling Climate at Ecologically
505 Relevant Scales. *Adv. Ecol. Res.* 58, 101–161
- 506 3 Scherrer, D. and Körner, C. (2010) Infra-red thermometry of alpine landscapes
507 challenges climatic warming projections. *Glob. Chang. Biol.* 16, 2602–2613
- 508 4 Chen, J. *et al.* (1999) Microclimate in forest ecosystem and landscape ecology:
509 Variations in local climate can be used to monitor and compare the effects of different
510 management regimes. *Bioscience* 49, 288–297
- 511 5 Porter, W.P. and Gates, D.M. (1969) Thermodynamic Equilibria of Animals with
512 Environment. *Ecol. Monogr.* 39, 227–244
- 513 6 Jones, H.G. (2014) *Plants and microclimate. A quantitative approach to environmental
514 plant physiology. Third Edition.*, Cambridge: Cambridge University Press.
- 515 7 Huey, R.B. *et al.* (2012) Predicting organismal vulnerability to climate warming: roles
516 of behaviour, physiology and adaptation. *Philos Trans R Soc L. B Biol. Sci.* 367, 1665–
517 1679
- 518 8 Kearney, M. and Porter, W. (2009) Mechanistic niche modelling: combining
519 physiological and spatial data to predict species' ranges. *Ecol. Lett.* 12, 334–350
- 520 9 Novick, K.A. *et al.* (2016) Cold air drainage flows subsidize montane valley ecosystem
521 productivity. *Glob. Chang. Biol.* 22, 4014–4027
- 522 10 Uvarov, B.P. (1931) Insects and climate. *Trans. R. Entomol. Soc. London* 79, 1–232
- 523 11 Penuelas, J. *et al.* (2013) Evidence of current impact of climate change on life: a walk
524 from genes to the biosphere. *Glob. Chang. Biol.* 19, 2303–2338
- 525 12 Aussenac, G. (2000) Interactions between forest stands and microclimate:
526 Ecophysiological aspects and consequences for silviculture. *Ann. For. Sci.* 57, 287–
527 301

- 528 13 Jucker, T. *et al.* (2018) Canopy structure and topography jointly constrain the
529 microclimate of human-modified tropical landscapes. *Glob. Chang. Biol.* 24, 5243-
530 5258
- 531 14 Maclean, I.M.D. *et al.* (2018) Microclima: an R package for modelling meso- and
532 microclimate. *Methods Ecol. Evol.* DOI: 10.1111/2041-210X.13093
- 533 15 WMO, World Meteorological Organization (2008) Guide to Meteorological Instruments
534 and Methods of Observation.
- 535 16 Suggitt, A.J. *et al.* (2011) Habitat microclimates drive fine-scale variation in extreme
536 temperatures. *Oikos* 120, 1–8
- 537 17 Bertrand, R. *et al.* (2011) Changes in plant community composition lag behind climate
538 warming in lowland forests. *Nature* 479, 517–520
- 539 18 Barnosky, A.D. *et al.* (2012) Approaching a state shift in Earth’s biosphere. *Nature*
540 486, 52–58
- 541 19 Devictor, V. *et al.* (2012) Differences in the climatic debts of birds and butterflies at a
542 continental scale. *Nat. Clim. Chang.* 2, 121–124
- 543 20 Dullinger, S. *et al.* (2012) Extinction debt of high-mountain plants under twenty-first-
544 century climate change. *Nat. Clim. Chang.* 2, 619–622
- 545 21 De Frenne, P. *et al.* (2013) Microclimate moderates plant responses to macroclimate
546 warming. *Proc. Natl. Acad. Sci.* 110, 18561–18565
- 547 22 Alexander, J.M. *et al.* (2018) Lags in the response of mountain plant communities to
548 climate change. *Glob. Chang. Biol.* 24, 563–579
- 549 23 Scherrer, D. and Körner, C. (2011) Topographically controlled thermal-habitat
550 differentiation buffers alpine plant diversity against climate warming. *J. Biogeogr.* 38,
551 406–416
- 552 24 Lenoir, J. *et al.* (2017) Climatic microrefugia under anthropogenic climate change:
553 implications for species redistribution. *Ecography.* 40, 253–266

- 554 25 Suggitt, A.J. *et al.* (2018) Extinction risk from climate change is reduced by
555 microclimatic buffering. *Nat. Clim. Chang.* 8, 713–717
- 556 26 Lenoir, J. *et al.* (2013) Local temperatures inferred from plant communities suggest
557 strong spatial buffering of climate warming across Northern Europe. *Glob. Chang.*
558 *Biol.* 19, 1470–1481
- 559 27 Potter, K.A. *et al.* (2013) Microclimatic challenges in global change biology. *Glob.*
560 *Chang. Biol.* 19, 2932–2939
- 561 28 Kearney, M.R. *et al.* (2014) Microclimate modelling at macro scales: a test of a general
562 microclimate model integrated with gridded continental-scale soil and weather data.
563 *Methods Ecol. Evol.* 5, 273–286
- 564 29 Maclean, I.M. *et al.* (2017) Fine-scale climate change: modelling spatial variation in
565 biologically meaningful rates of warming. *Glob. Chang. Biol.* 23, 256–268
- 566 30 Lefsky, M.A. *et al.* (2002) Lidar remote sensing for ecosystem studies. *Bioscience* 52,
567 19–30
- 568 31 Tymen, B. *et al.* (2017) Quantifying micro-environmental variation in tropical
569 rainforest understory at landscape scale by combining airborne LiDAR scanning and a
570 sensor network. *Ann. For. Sci.* 74, 32
- 571 32 Frey, S.J.K. *et al.* (2016) Spatial models reveal the microclimatic buffering capacity of
572 old-growth forests. *Sci. Adv.* 2:e1501392
- 573 33 Pradervand, J.-N. *et al.* (2014) Very high resolution environmental predictors in species
574 distribution models. *Prog. Phys. Geogr.* 38, 79–96
- 575 34 George, A.D. *et al.* (2015) Using LiDAR and remote microclimate loggers to
576 downscale near-surface air temperatures for site-level studies. *Remote Sens. Lett.* 6,
577 924–932
- 578 35 Greiser, C. *et al.* (2018) Monthly microclimate models in a managed boreal forest
579 landscape. *Agric. For. Meteorol.* 250–251, 147–158

- 580 36 Körner, C. and Hiltbrunner, E. (2018) The 90 ways to describe plant temperature.
581 *Perspect. Plant Ecol. Evol. Syst.* 30, 16–21
- 582 37 Westoby, M.J. *et al.* (2012) ‘Structure-from-Motion’ photogrammetry: A low-cost,
583 effective tool for geoscience applications. *Geomorphology* 179, 300–314
- 584 38 White, J. *et al.* (2013) The Utility of Image-Based Point Clouds for Forest Inventory: A
585 Comparison with Airborne Laser Scanning. *Forests* 4, 518–536
- 586 39 Fonstad, M.A. *et al.* (2012) Topographic structure from motion: a new development in
587 photogrammetric measurement. *Earth Surf. Process. Landforms* 38, 421–430
- 588 40 Milling, C.R. *et al.* (2018) Habitat structure modifies microclimate: An approach for
589 mapping fine-scale thermal refuge. *Methods Ecol. Evol.* 2018, 1648–1657
- 590 41 Anderson, K. and Gaston, K.J. (2013) Lightweight unmanned aerial vehicles will
591 revolutionize spatial ecology. *Front. Ecol. Environ.* 11, 138–146
- 592 42 Maes, W. *et al.* (2017) Optimizing the Processing of UAV-Based Thermal Imagery.
593 *Remote Sens.* 9, 476
- 594 43 Kong, F. *et al.* (2016) Retrieval of three-dimensional tree canopy and shade using
595 terrestrial laser scanning (TLS) data to analyze the cooling effect of vegetation. *Agric.*
596 *For. Meteorol.* 217, 22–34
- 597 44 Ehbrecht, M. *et al.* (2019) Effects of structural heterogeneity on the diurnal temperature
598 range in temperate forest ecosystems. *For. Ecol. Manage.* 432, 860–867
- 599 45 Hancock, S. *et al.* (2017) Measurement of fine-spatial-resolution 3D vegetation
600 structure with airborne waveform lidar: Calibration and validation with voxelised
601 terrestrial lidar. *Remote Sens. Environ.* 188, 37–50
- 602 46 Asner, G.P. *et al.* (2015) Quantifying forest canopy traits: Imaging spectroscopy versus
603 field survey. *Remote Sens. Environ.* 158, 15–27
- 604 47 Schneider, F.D. *et al.* (2017) Mapping functional diversity from remotely sensed
605 morphological and physiological forest traits. *Nat. Commun.* 8, 1441

606 48 Canham, C.D. *et al.* (1994) Causes and consequences of resource heterogeneity in
607 forests: interspecific variation in light transmission by canopy trees. *Can. J. For. Res.*
608 24, 337–349

609 49 Musselman, K.N. *et al.* (2013) Estimation of solar direct beam transmittance of conifer
610 canopies from airborne LiDAR. *Remote Sens. Environ.* 136, 402–415

611 50 Campbell, G.S. (1986) Extinction coefficients for radiation in plant canopies calculated
612 using an ellipsoidal inclination angle distribution. *Agric. For. Meteorol.* 36, 317–321

613 51 Alexander, C. *et al.* (2013) Airborne laser scanner (LiDAR) proxies for understory
614 light conditions. *Remote Sens. Environ.* 134, 152–161

615 52 Gastellu-Etchegorry, J.-P. *et al.* (2015) Discrete Anisotropic Radiative Transfer (DART
616 5) for Modeling Airborne and Satellite Spectroradiometer and LIDAR Acquisitions of
617 Natural and Urban Landscapes. *Remote Sensing* 7, 1667-1701

618 53 von Arx, G. *et al.* (2013) Microclimate in forests with varying leaf area index and soil
619 moisture: potential implications for seedling establishment in a changing climate. *J.*
620 *Ecol.* 101, 1201–1213

621 54 De Frenne, P. and Verheyen, K. (2016) Weather stations lack forest data. *Science* (80).
622 351, 234

623 55 Latimer, C.E. and Zuckerberg, B. (2016) Forest fragmentation alters winter
624 microclimates and microrefugia in human-modified landscapes. *Ecography.* 40, 158–
625 170

626 56 Pepin, N.C. *et al.* (2011) The influence of surface versus free-air decoupling on
627 temperature trend patterns in the western United States. *J. Geophys. Res.* 116,

628 57 Daly, C. *et al.* (2010) Local atmospheric decoupling in complex topography alters
629 climate change impacts. *Int. J. Climatol.* 30, 1857–1864

630 58 Ashcroft, M.B. and Gollan, J.R. (2013) Moisture, thermal inertia, and the spatial
631 distributions of near-surface soil and air temperatures: Understanding factors that

632 promote microrefugia. *Agric. For. Meteorol.* 176, 77–89

633 59 Leempoel, K. *et al.* (2015) Very high-resolution digital elevation models: are multi-
634 scale derived variables ecologically relevant? *Methods Ecol. Evol.* 6, 1373–1383

635 60 Kemppinen, J. *et al.* (2017) Modelling soil moisture in a high-latitude landscape using
636 LiDAR and soil data. *Earth Surf. Process. Landforms* DOI: 10.1002/esp.4301

637 61 Boudreault, L.-É. *et al.* (2017) How Forest Inhomogeneities Affect the Edge Flow.
638 *Boundary-Layer Meteorol.* 162, 375–400

639 62 Schlegel, F. *et al.* (2012) Large-Eddy Simulation of Inhomogeneous Canopy Flows
640 Using High Resolution Terrestrial Laser Scanning Data. *Boundary-Layer Meteorol.*
641 142, 223–243

642 63 Faye, E. *et al.* (2016) A toolbox for studying thermal heterogeneity across spatial
643 scales: from unmanned aerial vehicle imagery to landscape metrics. *Methods Ecol.*
644 *Evol.* 7, 437–446

645 64 Michaletz, S.T. *et al.* (2015) Plant Thermoregulation: Energetics, Trait-Environment
646 Interactions, and Carbon Economics. *Trends Ecol. Evol.* 30, 714–724

647 65 Möller, M. *et al.* (2007) Use of thermal and visible imagery for estimating crop water
648 status of irrigated grapevine. *J. Exp. Bot.* 58, 827–838

649 66 Jones, H.G. *et al.* (2009) Thermal infrared imaging of crop canopies for the remote
650 diagnosis and quantification of plant responses to water stress in the field. *Funct. Plant*
651 *Biol.* 36, 978–989

652 67 Senior, R.A. *et al.* (2018) Tropical forests are thermally buffered despite intensive
653 selective logging. *Glob. Chang. Biol.* 24, 1267–1278

654 68 Dugdale, S.J. *et al.* (2015) Spatial distribution of thermal refuges analysed in relation to
655 riverscape hydromorphology using airborne thermal infrared imagery. *Remote Sens.*
656 *Environ.* 160, 43–55

657 69 Leuzinger, S. and Körner, C. (2007) Tree species diversity affects canopy leaf

658 temperatures in a mature temperate forest. *Agric. For. Meteorol.* 146, 29–37

659 70 Vollmer, M. and Möllmann, K.-P. (2017) *Infrared Thermal Imaging: Fundamentals,*
660 *Research and Applications*, John Wiley & Sons.

661 71 Rubio, E. *et al.* (1997) Emissivity measurements of several soils and vegetation types
662 in the 8–14, μm Wave band: Analysis of two field methods. *Remote Sens. Environ.* 59,
663 490–521

664 72 Fick, S.E. and Hijmans, R.J. (2017) WorldClim 2: new 1-km spatial resolution climate
665 surfaces for global land areas. *Int. J. Climatol.* 37, 4302–4315

666 73 Karger, D.N. *et al.* (2017) Climatologies at high resolution for the earth’s land surface
667 areas. *Sci. Data* 4, 170122

668 74 Dingman, J.R. *et al.* (2013) Cross-scale modeling of surface temperature and tree
669 seedling establishment in mountain landscapes. *Ecol. Process.* 2, 30

670 75 McCullough, I.M. *et al.* (2016) High and dry: high elevations disproportionately
671 exposed to regional climate change in Mediterranean-climate landscapes. *Landsc. Ecol.*
672 31, 1063–1075

673 76 Meineri, E. and Hylander, K. (2017) Fine-grain, large-domain climate models based on
674 climate station and comprehensive topographic information improve microrefugia
675 detection. *Ecography.* 40, 1003–1013

676 77 Kearney, M.R. and Porter, W.P. (2017) NicheMapR – an R package for biophysical
677 modelling: the microclimate model. *Ecography.* 40, 664–674

678 78 Kearney, M.R. *et al.* (2014) microclim: Global estimates of hourly microclimate based
679 on long-term monthly climate averages. *Sci. Data* 1, 140006

680 79 Hannah, L. *et al.* (2014) Fine-grain modeling of species’ response to climate change:
681 holdouts, stepping-stones, and microrefugia. *Trends Ecolgy Evol.* 29, 390–397

682 80 Dobrowski, S.Z. (2011) A climatic basis for microrefugia: the influence of terrain on
683 climate. *Glob. Chang. Biol.* 17, 1022–1035

- 684 81 Kollas, C. *et al.* (2013) Spring frost and growing season length co-control the cold
685 range limits of broad-leaved trees. *J. Biogeogr.* 41, 773–783
- 686 82 Opedal, Ø.H. *et al.* (2015) Linking small-scale topography with microclimate, plant
687 species diversity and intra-specific trait variation in an alpine landscape. *Plant Ecol.*
688 *Divers.* 8, 305–315
- 689 83 Zellweger, F. *et al.* (2017) Beta diversity of plants, birds and butterflies is closely
690 associated with climate and habitat structure. *Glob. Ecol. Biogeogr.* 26, 898–906
- 691 84 Maclean, I.M.D. *et al.* (2015) Microclimates buffer the responses of plant communities
692 to climate change. *Glob. Ecol. Biogeogr.* 24, 1340–1350
- 693 85 Gauzere, P. *et al.* (2017) Where do they go? The effects of topography and habitat
694 diversity on reducing climatic debt in birds. *Glob Chang Biol* 23, 2218–2229
- 695 86 Milanesi, P. *et al.* (2017) Three-dimensional habitat structure and landscape genetics: a
696 step forward in estimating functional connectivity. *Ecology* 98, 393–402
- 697 87 Davies, A.B. and Asner, G.P. (2014) Advances in animal ecology from 3D-LiDAR
698 ecosystem mapping. *Trends Ecol. Evol.* 29, 681–691
- 699 88 Simonson, W.D. *et al.* (2013) Remotely sensed indicators of forest conservation status:
700 Case study from a Natura 2000 site in southern Portugal. *Ecol. Indic.* 24, 636–647
- 701 89 Zellweger, F. *et al.* (2016) Environmental predictors of species richness in forest
702 landscapes: abiotic factors versus vegetation structure. *J. Biogeogr.* 43, 1080–1090
- 703 90 Scheffers, B.R. *et al.* (2014) Microhabitats reduce animal’s exposure to climate
704 extremes. *Glob. Chang. Biol.* 20, 495–503
- 705 91 Nakamura, A. *et al.* (2017) Forests and Their Canopies: Achievements and Horizons in
706 Canopy Science. *Trends Ecol Evol.* 32, 438–451
- 707 92 Ashton, L.A. *et al.* (2016) Vertical stratification of moths across elevation and latitude.
708 *J. Biogeogr.* 43, 59–69
- 709 93 Lin, B.B. (2007) Agroforestry management as an adaptive strategy against potential

- 710 microclimate extremes in coffee agriculture. *Agric. For. Meteorol.* 144, 85–94
- 711 94 Lee, W.S. *et al.* (2010) Sensing technologies for precision specialty crop production.
712 *Comput. Electron. Agric.* 74, 2–33
- 713 95 Mulla, D.J. (2013) Author 's personal copy Special Issue : Sensing in Agriculture
714 Review Twenty five years of remote sensing in precision agriculture : Key advances
715 and remaining knowledge gaps 5. *Biosyst. Eng.* 114, 358–371
- 716 96 Faye, E. *et al.* (2017) Does heterogeneity in crop canopy microclimates matter for
717 pests? Evidence from aerial high-resolution thermography. *Agric. Ecosyst. Environ.*
718 246, 124–133
- 719 97 Frazer, G.W. *et al.* (2011) Simulated impact of sample plot size and co-registration
720 error on the accuracy and uncertainty of LiDAR-derived estimates of forest stand
721 biomass. *Remote Sens. Environ.* 115, 636–649
- 722 98 Metz, M. *et al.* (2014) Surface Temperatures at the Continental Scale: Tracking
723 Changes with Remote Sensing at Unprecedented Detail. *Remote Sensing* 6, 3822-3840
- 724 99 Moeser, D. *et al.* (2014) Canopy closure, LAI and radiation transfer from airborne
725 LiDAR synthetic images. *Agric. For. Meteorol.* 197, 158–168
- 726 100 Bennie, J. *et al.* (2008) Slope, aspect and climate: Spatially explicit and implicit models
727 of topographic microclimate in chalk grassland. *Ecol. Modell.* 216, 47–59

728

729 **Figure legends**

730 **Figure 1.** Conceptual overview of the approach used to generate microclimate maps from a sensor network. A:
731 Microclimate data are recorded using a network of sensors measuring air/soil temperature and humidity
732 conditions, e.g., placed in the open (S1) and below tree canopies (S2) as shown by 3D airborne Light Detection
733 and Ranging (LiDAR) data in the top panel. The microclimate data from each sensor (S1, S2, and black dots) are
734 then summarised in ecologically meaningful ways, e.g. to daily minimum (Tmin) and maximum (Tmax)
735 temperatures as shown in the middle left panel, and related to vegetation structure and the topography mapped
736 using remote sensing technologies, e.g., LiDAR, as shown for canopy height and elevation across a landscape in

737 the tropical lowlands [13]. B: Statistical models are then used to predict microclimate across the entire mapped
738 landscape and over time. In this example, maximum canopy height and topographic position were strong
739 predictors of maximum daily air temperatures in the understory (left), which explained small-scale variation
740 of maximum vapour pressure deficit (VPD) (right), as indicated by the black arrows (taken from Jucker et al.
741 [13]).

742

743 **Figure 2.** Thermal infrared (TIR) imaging reveals spatially detailed information about surface temperatures.
744 Images A and B show land surface temperatures (LSTs) for Europe (EuroLST) derived from freely available
745 MODIS satellite images with a pixel size of 250 m [98]. On the other hand, data for images C to E were recorded
746 at sub-metre resolution by an UAV flown at 70 m height above ground during an exceptional drought in June
747 2017 in a tree diversity experiment in Belgium (www.treedivbelgium.ugent.be). Panel C is conventional red-
748 green-blue (RGB) photography, panel D shows the vegetation height (m) determined by structure-from-motion
749 analysis of overlapping photos and panel E shows the surface temperature derived from the TIR image. We see
750 that surface temperatures of plants on the ground are considerably higher than those of tree surfaces, due to
751 different transpiration rates as a response to water shortage. The data was processed following Maes et al. [42].

752

753 **Box 1 Figure I.** Probability of occurrence maps based on a virtual species approach, for which the realized niche
754 is known, predicted with current-day macroclimate (A) and microclimate data (B), and projected into the future
755 under a 2 °C warming scenario (C and D respectively). The temperature data for images A and C refer to long-
756 term (30-yr averages during the period 1970-2000) maximum temperature of the warmest month and were
757 obtained by downscaling macroclimate at 25-m resolution to incorporate topoclimatic processes. Spatial
758 variation in microclimate (temperature in this case) generated by trees (i.e. canopy cover) and topography (i.e.
759 topographic concavity) were modelled using 50-cm resolution maps (images B and D) derived from 3D airborne
760 Light Detection and Ranging (LiDAR). Note that microclimatic models indicate much larger areas of suitable
761 habitat than macroclimatic models. In particular, many potential microrefugia are identified in image D which
762 could continue to provide suitable habitat under climate warming (adapted from Lenoir et al. [24]).

763

764 **Box 2 Figure I.** Using airborne Light Detection and Ranging (LiDAR) to map solar radiation fluxes in a
765 mountainous region. A: Potential clear sky solar radiation predicted to reach the ground on a summer day if
766 vegetation is absent (i.e. based on a digital terrain model generated by LiDAR); B: Forest canopy height
767 measured over the same region; C: Potential clear sky solar radiation calculated to reach the ground having

768 penetrated through the forest canopy, assuming an increase of shading with increasing vegetation cover and
769 height. It can be seen that much of the landscape is deeply shaded by trees and shrubs, making it suitable for
770 shade-tolerant plant species. D: 3D airborne LiDAR-derived elevation data of a forest (black rectangle in B) is
771 used to construct synthetic hemispherical images at 1 m and 25 m height above the forest floor [99]. E:
772 Reconstructed hemispherical images, taken at the red point position in B, show portions of the sky obscured by
773 trees (black) and the terrain (blue), from which diffuse and direct light transmission can be calculated. These
774 images can be calculated for any point in the landscape and at any height in forest canopies providing
775 unprecedented opportunities to estimate the microclimate in the neighbourhood of individual organisms. Note
776 that ground topography (elevation, aspect and slope) have strong influences on solar radiation [100], and high-
777 resolution DTMs from LiDAR surveys provide critical input data for quantifying these effects [13,14].

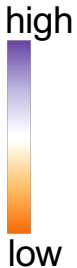
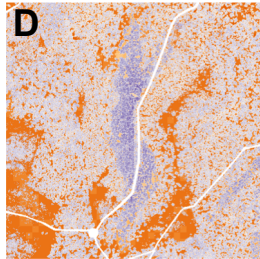
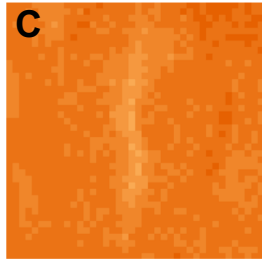
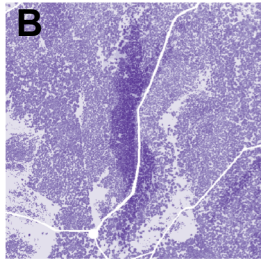
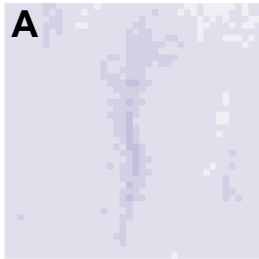
778

779 **Box 3 Figure I.** A: Weather stations as illustrated on the left provide long-term climate data for synoptic
780 conditions (right panel). B: Microclimate data from sensor networks (*cf.* Figure 1) are currently available mostly
781 for short time periods only, e.g. months to a few years (right panel). The left image shows a shielded sensor
782 placed on the north side of a tree trunk. C: Maximum air temperatures below canopies (i.e. microclimate) are
783 frequently offset by several degrees compared to free-air conditions (i.e. macroclimate) and the offset trend over
784 time may vary. Long-term data series are required to assess the differences in spatiotemporal dynamics between
785 macro- and microclimate (see text).

Probability of occurrence

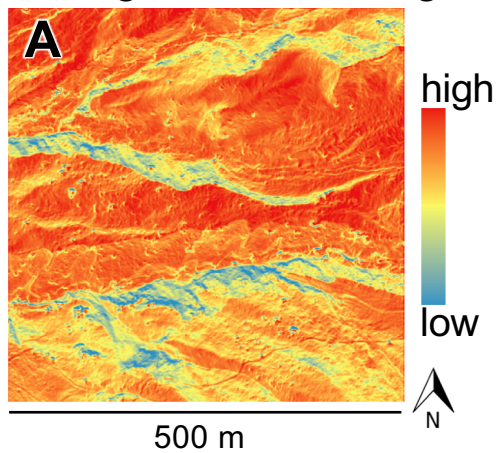
Current climate

Future climate (+2°C)

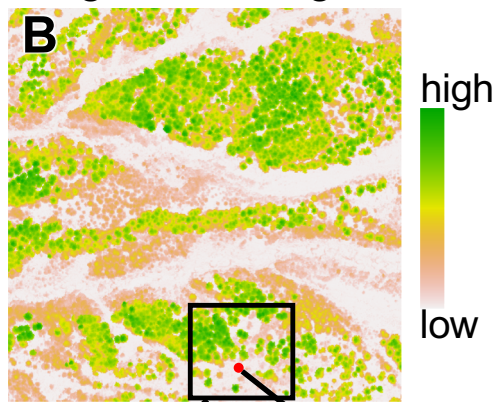


1 km

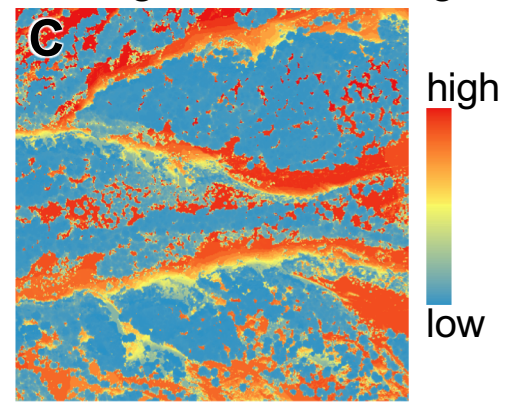
Radiation
w/o vegetation shading



Vegetation height

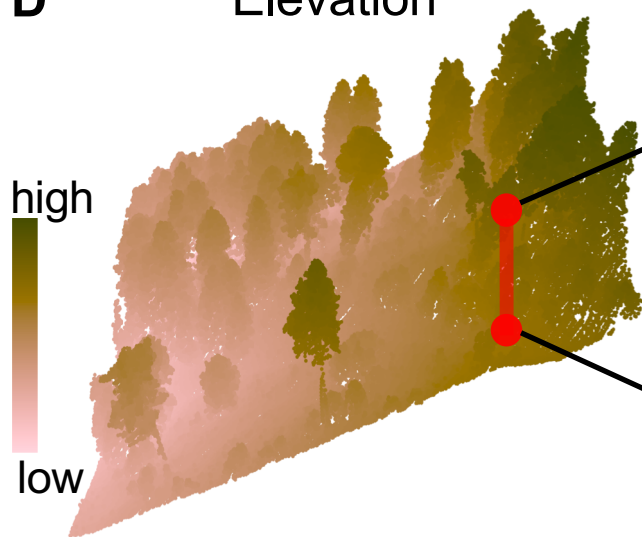


Radiation
with vegetation shading

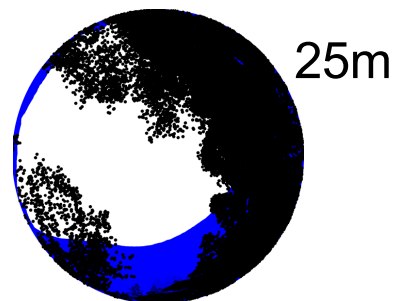


D

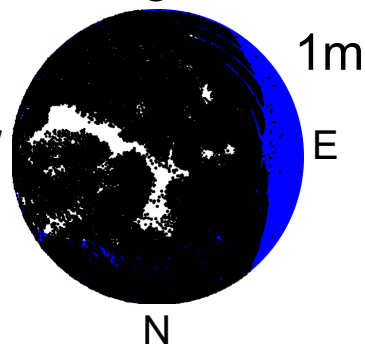
Elevation



E

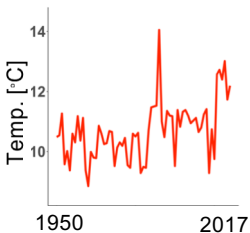


W

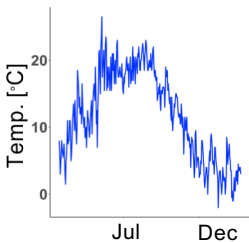
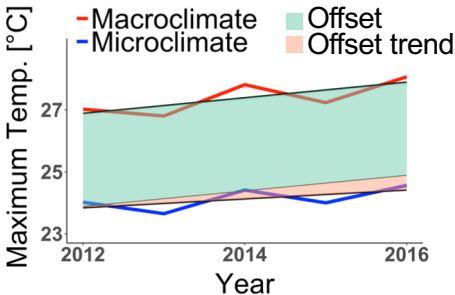


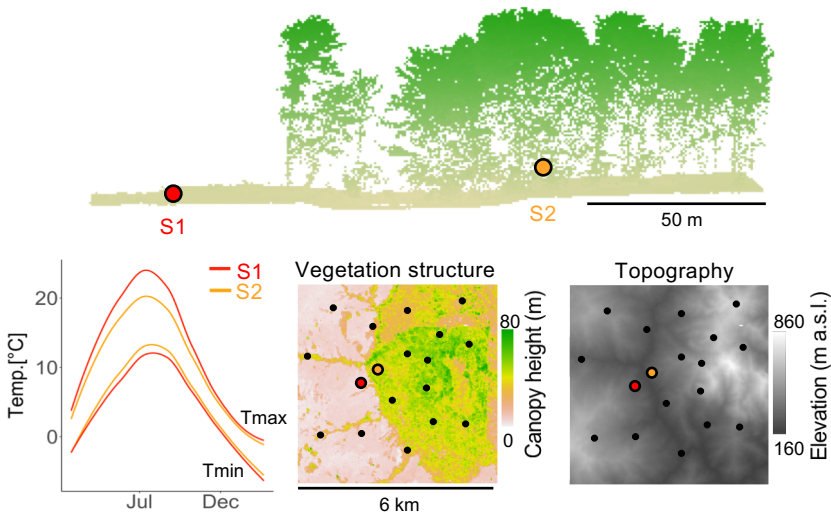
A

Weather Station

**B**

Microclimate sensor network

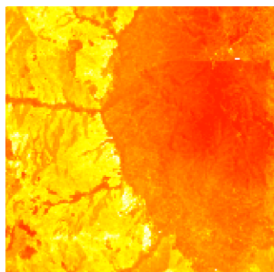
**C**

A Network of microclimate sensors within a laser-scanned woodland

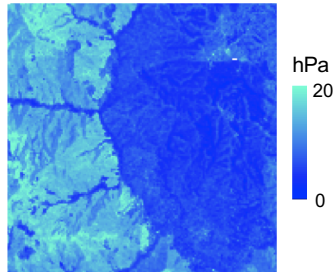
Relate summary statistic for each sensor (e.g. daily maximum and minimum temperatures) to structural information from remote sensing

**B** Calibrate and validate statistical models and use them to predict microclimate across the landscape

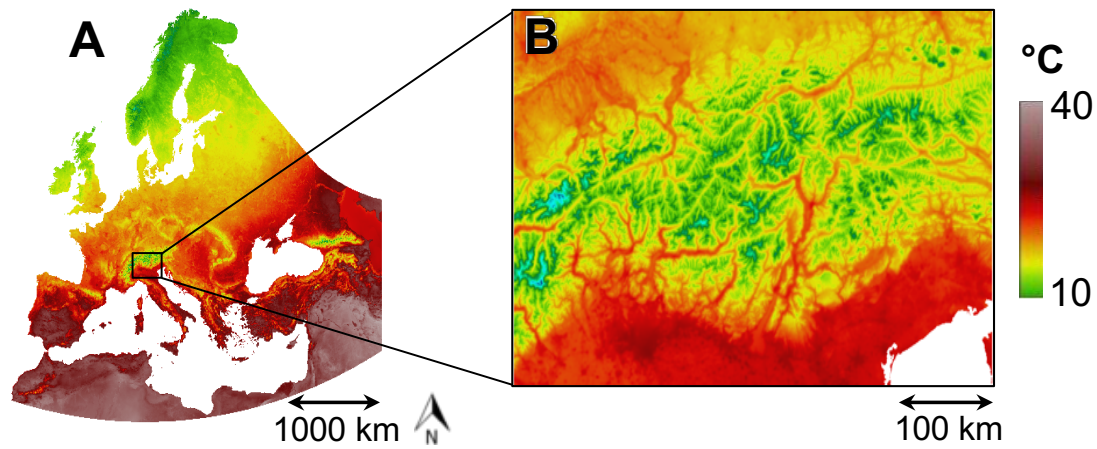
Maximum temperature



Maximum vapour pressure deficit



Satellite-based Land Surface Temperature (LST)



UAV-based remote sensing

